Discrete Row Growth at Vicinal Surfaces

Vittorio Marsico, Martial Blanc, Klaus Kuhnke, and Klaus Kern

Institut de Physique Expérimentale, Ecole Polytechnique Fédérale de Lausanne, CH-1015 Lausanne, Switzerland
(Received 2 August 1996)

Discrete row growth during the initial stage of molecular beam epitaxy of rare gases and metals on the vicinal Pt(997) surface has been observed. The row-by-row growth is revealed by intensity oscillations in thermal-energy atom scattering at grazing incidence. Thermodynamic modeling provides an estimate of the excess binding energy close to the step edges.   [S0031-9007(96)01999-0]

Manipulating the morphology of epitaxial films through detailed control of the growth kinetics has attracted much interest recently. A primary goal is the layer-by-layer growth of smooth films with abrupt interfaces. The most widely used techniques for monitoring the growth mode are diffraction techniques [1–4], where the occurrence of intensity oscillations provides unique evidence for the desired two-dimensional (2D) growth. These oscillations in the diffracted or specularly reflected intensity reflect the periodically varying step density of homogeneously nucleating and successively coalescing 2D islands.

The presence of substrate steps can suppress the homogeneous nucleation on terraces in favor of heterogeneous step nucleation still permitting smooth two-dimensional growth. Binding energies for adatoms at step sites are in general larger than on terrace sites due to the increased coordination. As a consequence 2D islands preferentially nucleate at steps if the average adatom diffusion length is larger than the terrace width [5–7]. In the submonolayer range this can be exploited to grow quasi-one-dimensional systems like quantum wires using substrate step arrays as a template [8,9]. Similar to the growth mode classification in thin film epitaxy different step decoration modes can be distinguished, the occurrence of which depend on the detailed interaction of the adsorbate with the substrate step [10].

In the present Letter we demonstrate that the step decoration modes can be studied by specular thermal energy helium scattering at grazing incidence. For a regularly stepped Pt(997) surface we find during the adsorption of rare gases and during the deposition of metals in the submonolayer range oscillations in the reflected helium intensity. These intensity oscillations reflect the sequential growth of rows at the steps (named here discrete row growth or row-by-row growth) during deposition.

The vicinal Pt(997) surface, consisting of about 20 Å wide (111) terraces separated by $(11\bar{1})$ monatomic steps, has been chosen as substrate because it is known to exhibit a regular step-terrace ordering with a narrow terrace width distribution [11,12]. The initial growth of the rare gas Xe and the metal Ag on this surface has been

studied with a novel triple axis He-surface spectrometer [13] in grazing incidence scattering geometry. While the rare gases are adsorbed on the Pt(997) surface from the ambient gas phase, silver is deposited with a molecular beam effusion cell.

Xe films on Pt(997) grow in a 2D growth mode. This can be seen from the oscillations in specularly reflected He intensity shown in Fig. 1 (note that the scattering geometry is far from grazing incidence and specular to the (111) terraces). As is well known from the literature [2,3,14] each intensity maximum corresponds to the completion of a xenon layer. The damping of the oscillations is mainly due to the large Debye-Waller
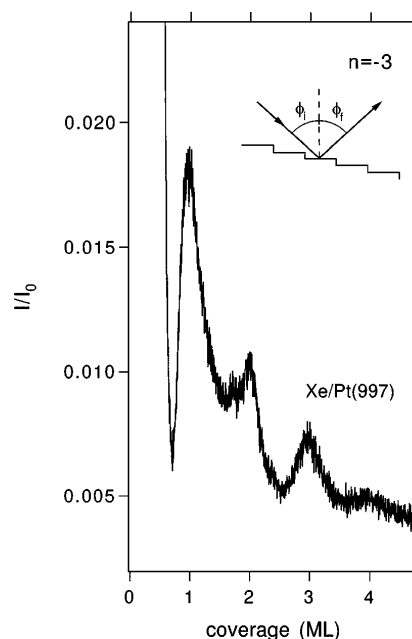

FIG. 1. He scattering intensity normalized to the intensity at zero coverage as a function of Xe coverage at nongrazing angles. Incidence angle of the He beam with respect to the surface normal $\theta_i = 53.9°$, exit angle $\theta_f = 41.0°$. The geometry corresponds to specular reflection with respect to substrate terraces, $\phi_i = \phi_f$, and a diffraction order $n = -3$ with respect to terrace periodicity. Xe ambient pressure 1.7×10^{-8} mbar, surface temperature $T = 34$ K, He beam wavelength $\lambda_{He} = 1.03$ Å.

factor of Xe multilayers. The measurement in Fig. 1 can be used to calibrate the coverage by the maxima of the layer-by-layer oscillations. The Xe monolayer is found to correspond to a coverage of $\Theta \approx 0.33$ [15].

At grazing incidence intensity oscillations are observed already in the submonolayer range. This is shown in Fig. 2 for Xe adsorption at 40 K. As will be discussed below, these oscillations result from a row-by-row attachment of adsorbates at the steps. A second system which exhibits oscillations due to discrete row growth is the Ag/Pt(997) system as is demonstrated by the second curve in Fig. 2. This metal on metal system has different physical and chemical properties than the physisorption system discussed above. It exhibits on Pt(111) pseudomorphic growth with an adatom density equal to the substrate atom density [16]. At 350 K we observe again the characteristic He intensity oscillations with a pronounced maximum at coverages of approximately one eighth of a monolayer and a shoulder at approximately two eighths, corresponding to the sequential growth of two rows. The submonolayer He reflectivity oscillations are most pronounced at grazing incidence close to 90°, diminish upon decreasing the incidence angle, and finally disappear at around 70° [17]. The intensity of the individual peaks depends strongly on the scattering geometry. For Xe/Pt(997) in Fig. 2 the geome-
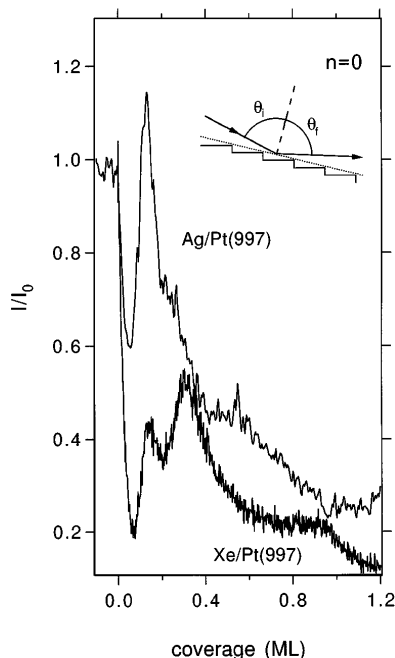

FIG. 2. Specular He scattering intensity at grazing angles as a function of Ag coverage (top) and Xe coverage (bottom). Ag: surface temperature $T = 350$ K, $\theta_i = \theta_f = 85.0°$, $\lambda_{He} = 0.97$ Å. Xe: surface temperature $T = 40$ K, $\theta_i = \theta_f = 76.2°$, $\lambda_{He} = 1.14$ Å. Note that in the grazing scattering geometry the incident and reflected He beams are specular to the macroscopic surface normal (i.e., diffraction order $n = 0$).

try was chosen to maximize the intensity in the second row peak.

Discrete row growth is the only plausible explanation for the oscillations. First, the two discussed systems are known to exhibit step decoration. Island formation on the narrow terraces can be excluded at the temperatures of the experiments. Thus preferential adsorption at the step will occur. Second, the observed oscillations are no interference effect because the coverage value at the maxima is found to be independent of geometry.

The observation of discrete row growth is specific to vicinal surfaces. Its clear observation depends on the presence of a sufficiently high step density and a regular step-terrace ordering as will be discussed below. At appropriate surface temperature the adatom mobility is high enough on the terraces to allow migration to the steps. Once attached to the steps the mobility is reduced. Because of the random nucleation of 1D nuclei the defect (kink) density increases in the beginning of the step decoration resulting in a decrease of reflected He intensity. During further attachment of atoms to the step the 1D nuclei grow laterally and finally coalesce to form a row of decreasing defect density. For a completed row the defect density reaches a minimum resulting in an intensity maximum.

The similarity of the oscillations exhibited by the two systems—Xe and Ag on Pt(997)—suggests similar step edge decoration in the two cases. It is known that in the case of Ag the attachment occurs exclusively at the bottom of steps [7]. Recent scanning tunneling microscopy studies of Xe adsorption on Pt(111) have suggested that Xe might preferentially bind at upper edges of isolated steps [18]. We found that this is unlikely for Xe growth at the vicinal Pt(997) surface. A detailed diffraction study for one and two complete Xe rows shows a shift of the diffraction intensity envelope function towards larger diffraction angles with respect to the clean surface [19]. This indicates a reduction of terrace bending [11] only consistent with Xe decoration of the lower step edges.

Because of the increased coordination of the adsorbate at the lower step edge, the adsorption energy is higher at the step than on the terrace. After the formation of a complete row adsorption can continue by the attachment of further rows depending on the adsorbate—adsorbate interaction potential and the range of the adsorbate—step interaction potential. The result is a more or less complete row-by-row growth resulting in a sequence of He intensity oscillations. The row oscillations for the two systems presented in this Letter disappear after two rows (Fig. 2). The main reason is the decreasing adsorbate-step interaction strength. In the physisorption system Xe/Pt(997), for example, one can assume that the difference in binding energy for an atom in row n and in row $n + 1$ decreases with increasing n. As a result, at a given temperature the row-by-row growth will become less strict. Thermodynamically discrete row

growth is favored with decreasing temperature [10]. At too low temperature, however, the decreased mobility of the adatoms and the finite adsorbate flux will finally obstruct any row-by-row growth. It can be concluded that row-by-row growth will be observable for a given row number n only over a limited temperature range. The fact that the same growth mode is observed for two qualitatively different adsorbate systems in different temperature ranges underlines the generality of the growth mechanism.

The oscillations will only be perfectly observable for substrate surfaces with equidistant steps. For a homogeneous deposition rate the uptake of adsorbates is higher on wider terraces than it is on narrower ones and the first and further rows will be completed on wider terraces earlier than on narrower ones. As a result the intensity maxima will smear out with increasing coverage because the terrace width exhibit a distribution function of finite width. For a coverage of more than half a monolayer, however, the peak broadening will reduce again and—apart from statistical fluctuations in the adsorption—the monolayer coverage is reached on all terraces at the same time. Thus for real surfaces the visibility of discrete row growth is best just above and below integer layer coverages.

We have further studied row-by-row growth with respect to its thermodynamic properties. Figure 3 shows adsorption measurements for a Xe gas pressure of 3×10^{-8} mbar at different surface temperatures. At this pressure Xe multilayer adsorption occurs below 57 K and monolayer adsorption below 91 K [19]. It can be seen from Fig. 3 that at 100 K adsorption ends exactly on the first peak. When the first row is complete, equilibrium with the gas phase is attained and no further adsorption takes place. A similar control of second row formation would require a precise temperature adjustment because of the small difference in binding energy between the second and further rows.

In order to estimate step binding energies for the Xe/Pt(997) system we first deposited a certain number of Xe rows at 40 K. The exact dosing was controlled by the intensity variations in the reflected He beam. By temperature variation a controlled desorption of adsorbate atoms from the step onto the terrace and a recondensation at the step is then performed. The process can be followed by specular He scattering under grazing incidence due to the change in diffuse scattering of the He beam. Figures 4(a) and 4(b) show repeated heating/cooling ramps for an initial coverage of one and two rows, respectively. For the second row a reversible variation of reflected He intensity is observed [Fig. 4(b)]. The first row, however, is more strongly bound to the step and atoms do not detach from the step below the temperature where also desorption from the surface occurs. As a result, no change in reflected He intensity can be observed [Fig. 4(a)] below Xe desorption temperature.
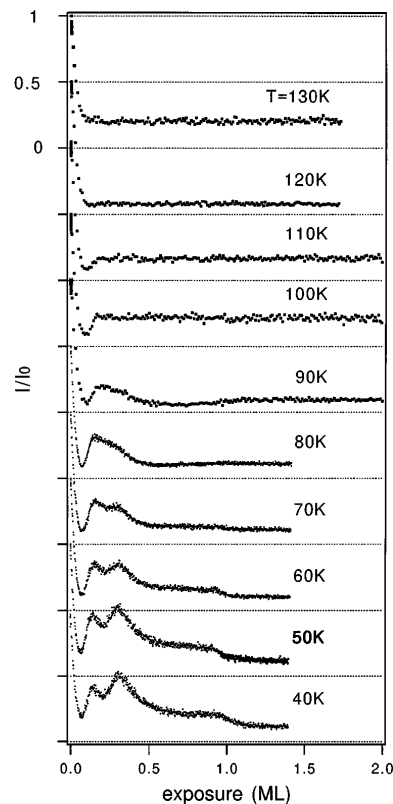

FIG. 3. Normalized specular He intensity in grazing incidence geometry $\theta_i = \theta_f = 76.2°$ ($n = 0$) as a function of Xe exposure of Pt(997) at different surface temperatures. In the range of Xe monolayer adsorption, $T < 90.9$ K, the exposure scale is identical to coverage. Ambient Xe pressure 3×10^{-8} mbar, $\lambda_{He} = 1.03$ Å.

The experiment can be interpreted quantitatively within the frame of a simplified potential model. Adsorbate atoms leaving a complete row increase the diffusely scattering defect concentration first as adatoms on the terrace and second as missing atoms in a complete row. These two contributions are added together to give an effective cross section for diffuse scattering Σ. The probability of terrace site occupation is reduced with respect to step site occupation by a Boltzmann factor containing the excess binding energy in row n defined as the energy difference ΔE_n between a site in row n and a terrace site far from the steps. The overall probability to find an atom on the terrace is increased due to the larger number of terrace sites compared to the number of step sites. In our simplified model we consider a Xe structure where a single adsorbate [3] atom is restricted to a cell of terrace width (20 Å) and two Pt nearest neighbor distances length (5.5 Å) [21]. We assume one site in a row per 14 and 21 sites on the terrace for the models of first and second row dynamics, respectively. Effects due to the interaction between adsorbate atoms are neglected. With the two free parameters Σ and ΔE_n the specularly reflected He intensity as a function of temperature is
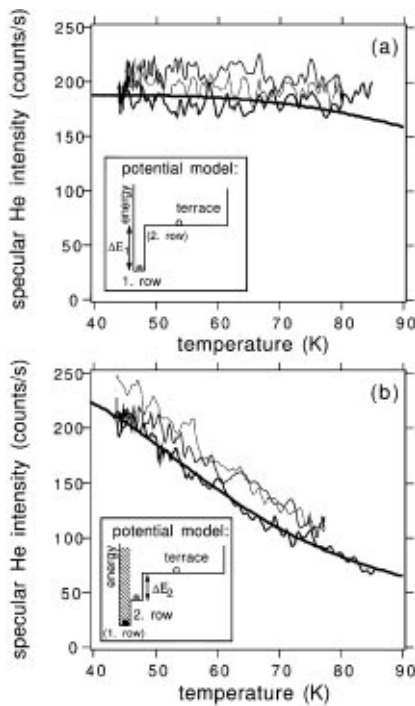
FIG. 4. Specular reflected He intensity at grazing incidence geometry during temperature sweeps after adsorption of one row (a) and two rows (b) of Xe. The jagged lines represent the measurements; the thickest lines are fits according to the model described in the text. The temperature range was chosen to avoid adsorbate desorption. The equilibrium situation and the absence of desorption are demonstrated by the reproducibility of the behavior in the successive upward-downward-upward temperature ramps coded by increasing line thickness. Insets: potential schemes employed for fitting (see text).

obtained as

$$I(T) = I_0 \Big[1 - \frac{n_s}{n_t \exp(\Delta E_n / kT) + n_s} \Big]^{n_t \Sigma}, \quad (1)$$

where n_s is the density of terrace adsorption sites and n_t is the density of atoms in the completed row.

In a first step we fit function (1) to the measurement for two rows coverage [thick line in Fig. 4(b)] assuming that the first row stays completely occupied and that the third and higher rows are degenerate in energy [inset Fig. 4(b)]. We obtain the best fit parameters $\Delta E_2 = 18$ meV and $\Sigma = 195$ Å^2. As can be expected from geometrical reasons the Σ value is larger than the cross sections of Xe adatoms on Pt(111) at less grazing geometry ($\Sigma = 120$ Å^2 for $\lambda_{He} = 0.57$ Å, $\theta_i = 40°$ [14]). In the next step we utilize the value for Σ in order to fit the behavior in the case of one adsorbed row. Assuming that the second and higher rows are degenerate [inset Fig. 4(b)], we obtain a lower limit for the excess binding energy of $\Delta E_1 > 40$ meV. With respect to the terrace adsorption energy in the first layer Xe/Pt(111) of 277 meV [15], the first and second rows thus exhibit an excess binding

energy of >14% and 7%, respectively. These values are comparable to estimates from isosteric heat measurements for Xe adsorption on vicinal Pd surfaces [20]. A more detailed interpretation of discrete row growth requires a sophisticated model for adsorbate-substrate interaction. Such a detailed study is currently in progress [21].

In conclusion, we demonstrated a novel experimental approach for the *in situ* study of step decoration. The observed discrete row growth and its real time monitoring with grazing incidence He scattering opens up the way for the fabrication of ultimate 1D superlattices with atomic scale periodicity.

We thank Rolf Schuster for enlightening discussions.

[1] J. J. Harris, B. A. Joyce, and P. J. Dobson, Surf. Sci. Lett. **103**, L90 (1981).
[2] L. J. Gomez, S. Bourgeal, J. Ibanez, and M. Salmeron, Phys. Rev. B **31**, 255 (1985).
[3] R. Kunkel, B. Poelsema, L. K. Verheij, and G. Comsa, Phys. Rev. Lett. **65**, 733 (1990).
[4] E. Vlieg, A. W. Denier van der Gon, J. F. Van der Veen, J. E. MacDonald, and C. Norris, Phys. Rev. Lett. **61**, 2241 (1988).
[5] G. A. Bassett, Philos. Mag. **3**, 1042 (1958).
[6] H. Bethge, Surf. Sci. **3**, 33 (1964).
[7] H. Röder, H. Brune, J.-P. Bucher, and K. Kern, Surf. Sci. **298**, 121 (1993).
[8] P. M. Petroff, A. C. Gossard, and W. Wiegmann, Appl. Phys. Lett. **45**, 620 (1984).
[9] Y. W. Mo and F. J. Himpsel, Phys. Rev. B **50**, 7868 (1994).
[10] J. Merikoski, J. Timonen, and K. Kaski, Phys. Rev. B **50**, 7925 (1994).
[11] G. Comsa, G. Mechtersheimer, B. Poelsema, and S. Tomoda, Surf. Sci. **89**, 123 (1979).
[12] E. Hahn, H. Schief, V. E. Marsico, A. Fricke, and K. Kern, Phys. Rev. Lett. **72**, 3378 (1994).
[13] H. Schief, Ph.D. thesis, Ecole Polytechnique Féderale de Lausanne, 1995.
[14] B. Poelsema and G. Comsa, *Scattering of Thermal Energy Atoms* (Springer-Verlag, Berlin, Heidelberg, 1989).
[15] K. Kern, R. David, P. Zeppenfeld, and G. Comsa, Surf. Sci. **195**, 353 (1988).
[16] H. Brune, H. Röder, C. Boragno, and K. Kern, Phys. Rev. B **49**, 2997 (1994).
[17] M. Blanc, V. E. Marsico, K. Kuhnke, and K. Kern (to be published).
[18] P. Zeppenfeld, S. Horch, and G. Comsa, Phys. Rev. Lett. **73**, 1259 (1994).
[19] V. E. Marsico, Ph.D. thesis, Ecole Polytechnique Féderale de Lausanne, 1995.
[20] R. Miranda, S. Daiser, K. Wandelt, and G. Ertl, Surf. Sci. **131**, 61 (1983).
[21] V. Pouthier, C. Ramseyer, C. Girardet, K. Kuhnke, V. Marsico, M. Blanc, R. Schuster, and K. Kern (to be published).